Acta Polytechnica CTU Proceedings **18**:66–71, 2018
doi:10.14311/APP.2018.18.0066

available online at http://ojs.cvut.cz/ojs/index.php/app

EXPERIMENTAL INVESTIGATION OF THE FAILURE BEHAVIOUR OF POLYPROPYLENE COMPOUNDS FOR INSTRUMENTED PUNCTURE TESTS

Florian Kiehas[a,*], Anna Kalteis[a], Michael Jerabek[b], Zoltán Major[a]

[a] *Institute for Polymer Product Engineering, Altenberger Straße 69, 4040 Linz, Austria*

[b] *Borealis Polyolefine GmbH, Sankt-Peter-Straße 25, 4020 Linz, Austria*

[*] corresponding author: florian.kiehas@jku.at

Abstract. Instrumented puncture tests according to ISO 6603-2 and ASTM D3763 were executed for five different Polypropylene compounds (talcum-, glass fibre- and elastomer modified) with specimen thicknesses ranging from 1 mm to 4 mm. Over 1500 puncture tests were executed at the *Impact & Long-term Behaviour* laboratory of the company *Borealis*® in Linz. This serves as strong foundation for statistical evaluations of the ductile/brittle transition temperature. For different materials and ductile/brittle transition determination methods, similar trends have been observed, which were characterized by introducing shift factors.

Keywords: polypropylene, compound, puncture, mechanical testing, ductile/brittle transition.

1. Introduction

For polymers, the energy absorption capacity strongly depends on the morphology of the plastic and the experimental environment. In the case of impact or puncture tests, temperature and strain rate variations have a significant influence on the failure behaviour: Almost all unoriented plastics exhibit brittle behaviour at low temperatures as well as at high strain rates [1].

Mechanical measurements of different puncture test standards result in distinct force-deflection curves, which in turn give different transitions from ductile to brittle. Furthermore, there is no concise method for the calculation of an exact transition temperature. It is assumed to be somewhere in the transition regime, a temperature range where sudden drops in energy absorption capacity indicate a change of impact behaviour from ductile to brittle. First, a precise method for the calculation has to be introduced. Then, the difference of the transition as a function of specimen thickness, temperature, test standard and other parameters can be determined.

2. Experimental Investigation

2.1. Test Parameters

The test setup and parameters of ISO 6603-2 and ASTM D3763 vary greatly. The main difference is the striker- and support ring geometry. For this reference analysis, tests for both standards were executed clamped, lubricated and at a speed of 4400 mm/s to allow for comparison. Therefore, the ASTM D3763 was slightly modified. A summary of all parameters can be looked up in Table 1 and Figure 1 shows the different geometries of each test standard. A more detailed description of each test standard can be looked up in literature [2, 3].

	ISO	**modified*** ASTM
Specimen dimensions	60×60 mm	⌀102 mm
Specimen thickness	1,2,3 mm	**1,2,3,4 mm***
Striker diameter	20.0 mm	12.7 mm
Support ring diameter	40.0 mm	76.0 mm
Test speed	4400 mm/s	**4400 mm/s***
Clamped	yes	yes
Lubricated	yes	**yes***

Table 1. Selected test conditions and parameters.

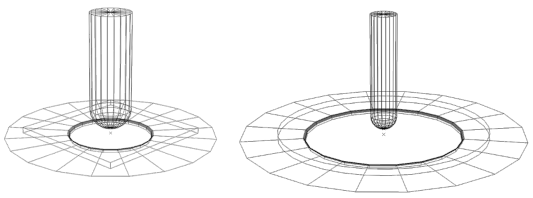

Figure 1. Striker and support ring geometries ISO (left) and ASTM (right).

2.2. Materials and test schedule

An extensive test program with a total number of 1586 specimens was carried out. The workload was divided between two machines: a servohydraulic *ROELL/AMSLER High Speed* and a gravitative (spring driven) *CEAST Fractovis Plus*. The comparability of measurement data obtained by both machines is documented by [4].

Five different polypropylene grades developed and produced by the company *Borealis*® were selected for this analysis. Three materials are in-reactor made heterophasic copolymers, which are different in rubber- and matrix design (elastomer modified polypropylene M1 to M3). M5 is also an in-reactor made heterophasic copolymer filled with talc. M4 is a glass filled polypropylene.

Four specimen thicknesses from 1 mm to 4 mm were tested with the exception of 4 mm ISO 6603-2 specimens, for which no injection moulding tool was available for manufacturing. 1 mm thick glass-fibre reinforced ISO plaques were also not available. Examined conditioning temperatures range from -70 °C to 23 °C. Eight temperature levels with five repetitions respectively were executed for each material, test standard and specimen thickness. In certain cases, additional measurements with three repetitions were carried out in the transition regime. Altogether, there are 34 test series with descriptions following Table 2:

Polypropylene compound	Test standard	Thickness
M1(Elastomer modified PP)	**ISO**(ISO 6603-2)	**t1**(1mm)
M2(Elastomer modified PP)	**ASTM**(ASTMD3763)	**t2**(2mm)
M3(Elastomer modified PP)		**t3**(3mm)
M4(Glass fibre reinforced PP)		**t4**(4mm)
M5(Talcum reinforced PP)		

TABLE 2. Nomenclature of test series.

For example, M4ASTMt3 represents a test series of material M4 with 3 mm thick specimens tested under the modified ASTM D3763 standard conditions.

2.3. DATA EVALUATION

For both test standards, the failure criterion is 50 % force drop after peak load F_m. The corresponding puncture energy E_p is obtained by integrating the force up to the deflection at puncture s_p.

The transition from elastic to elastic-plastic material behaviour was described with the introduction of a yield equivalent point (s_y/F_y)[5, 6]. The initial slope k_{lin} (corresponding to the relative stiffness [3]) of the curve can be approximated through the specification of another characteristic data point (s_{y0}/F_{y0}), which is necessary to avoid deviations caused by discontinuities at the start of impact. These points are defined as having the largest orthogonal distance from the direct connection line between origin (0/0) and peak load (s_m/F_m).

Thus, the energy E_m expended up to the maximum load can be split into an elastic part E_{el} and a plastic part E_{pl}. The graphical determination of the starting and end point of the initial slope, as well as the geometric interpretation of the plastic and elastic energy contributions are illustrated in Figure 2. Following characteristic values are examined:

- **Maximum force/deflection/energy** $F_m/s_m/E_m$
- **Puncture force/deflection/energy** $F_p/s_p/E_p$
- **Initial force/deflection** F_{y0}/s_{y0}
- **Yield equivalent force/deflection** F_y/s_y
- **Elastic/inelastic energy portions** E_{el}/E_{pl}
- **Relative stiffness** k_{lin}
- **Width of plastic plateau** Δs_w

$$k_{lin} = \frac{F_y - F_{y0}}{s_y - s_{y0}} \tag{1}$$

$$E_{el} = \frac{F_m^2}{2k_{lin}} \tag{2}$$

$$E_{pl} = E_m - E_{el} \tag{3}$$

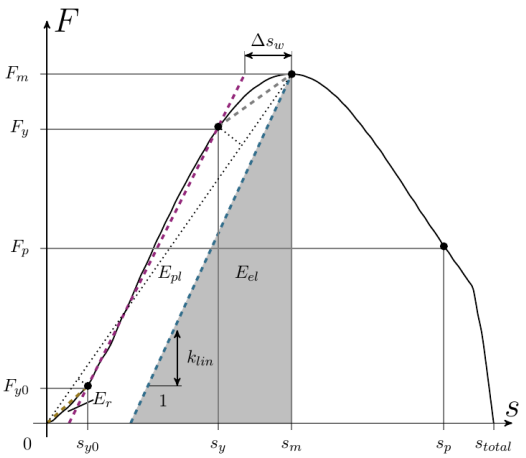

FIGURE 2. Evaluation of force-deflection data.

Two characteristic energy ratios have been introduced to describe the elastic properties as well as the failure behaviour of force-deflection data: the elastic energy ratio R_{el} and the ductility index [7] R_{duc} are specified in the following equations:

$$R_{el} = \frac{E_{pl} + E_{el}}{E_{el}} \tag{4}$$

$$R_{duc} = \frac{E_p - E_m}{E_p} \tag{5}$$

2.3.1. CURVE CHARACTERIZATION

The ISO 6603-2 curve type evaluation is a common method to characterize the force/deflection data obtained by puncture test ecperiments. It provides four typical types of curve progression that can usually be observed during data evaluation. In general, these range from ductile to brittle and focus on information like yielding, crack initiation and crack propagation [2]. Obtained data has been divided into these four categories, which are compiled in Figure 3.

The determination of the ductile/brittle transition by means of curve type characterization is described in section 2.4.5.

2.3.2. OPTICAL CHARACTERIZATION

The different types of fracture appearance are taken from a company-internal standard developed by General Motors Corporation. It grades fracture appearances from 1 to 11 and covers almost all kinds of break that may occur during impact testing. A subdivision ranging from ductile, to semi-ductile, up to brittle can be made. Illustrations of the individual fracture types are depicted in Figure 4.

The optical characterization was utilized to determine the ductile/brittle transition as well, which is described in section 2.4.6.

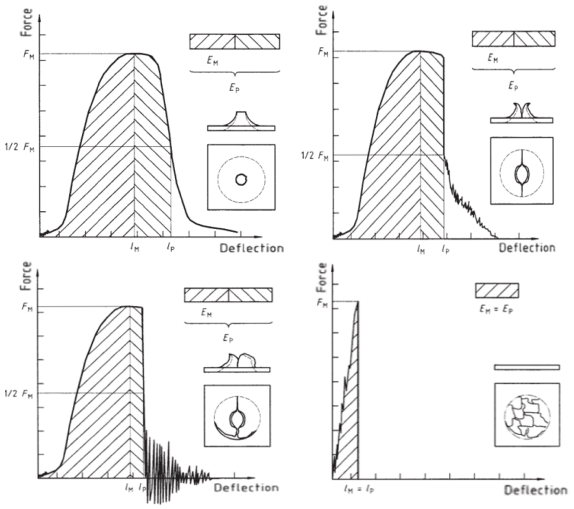

Figure 3. Curve types: YD *Yielding with deep drawing* (top left), YS *Yielding with stable crack* (top right), YU *Yielding with unstable crack* (bottom left), NY *No yielding* (bottom right) [2].

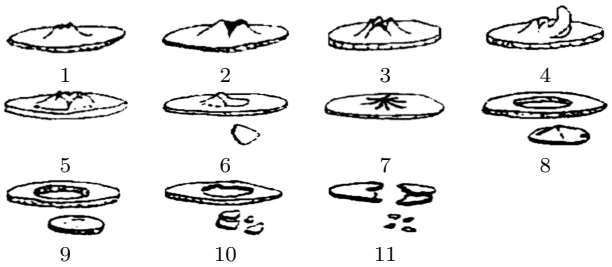

Figure 4. Fracture appearances: from *ductile* (1 - 5), to *ductile-fragile* (6 - 7), to *fragile-ductile* (8 - 9), up to *fragile* (10 - 11).

2.4. Ductile/brittle transition temperature

Various methods for the determination of the ductile/brittle transition temperature have been proposed in literature. For impact tests with steep inclines in the transition regime, not only the tangent formation of the upper- and lower shelf impact strengths [8, 9] but also optical investigations of the fracture appearance was investigated [10]. In [11] the inflection point of the temperature-dependent course was determined. Likewise, the penetration energy was proposed for exploration.

For this reference analysis, six different methods for the determination of the ductile/brittle transition temperature have been introduced and will be listed in the following subsections. It should be pointed out, that values are interpolated between data points. Figure 5 depicts graphic representations for the determination of each transition temperature.

2.4.1. Puncture energy

The arithmetic mean of the local minimum and maximum puncture energy E_p is calculated and the transition is assumed at the corresponding condition temperature T^E.

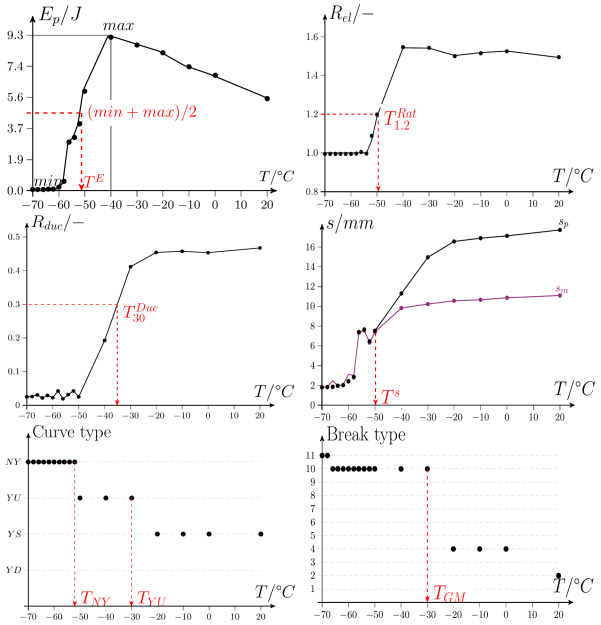

Figure 5. Determination of transition temperatures.

2.4.2. Elastic energy ratio

The peak load energy E_m is compared to the elastic energy E_{el}. It should be pointed out that the minimum value for this energy ratio is 1 when the plastic portion disappears. This case corresponds to absolutely no yielding before peak load with the corresponding curve type NY *No yielding*. Threshold values of 1.4, 1.2 and 1.0 were examined, with $T^{Rat}_{1.2}$ giving the most consistent results.

2.4.3. Ductility index

In contrast to the elastic energy ratio R_{el}, the ductility index R_{duc} is only obtained from information of the force deflection data after peak load. Therefore, yielding before peak load can not be detected with this method and is neglected. A ductility index of 0 implies, that the peak load is directly followed by an unstable crack, and consequently brittle fracture. Threshold values of 40 %, 30 % and 5 % were examined, with T^{Duc}_{30} giving the most consistent results.

2.4.4. Deflection

For completely brittle fractures, all characteristic events of a puncture test happen in a narrow time frame. The deflection difference between s_m, s_p and s_{total} (as well as s_y when there is no plastic plateau) becomes very small. T^s is the temperature where s_m and s_p converge.

2.4.5. Curve characterization

This method for the ductile/brittle transition temperature determination takes advantage of the elaborate ISO6603-2 curve characterization introduced in section 2.3.1. The curve types usually occur in the sequence of YD, YS, YU and NY from high to low

temperatures. An attempt was made to describe the ductile/brittle behaviour by looking out for the transitions from YU *Yielding with unstable crack* (bottom left) to NY *No yielding*. This leads to two specific temperatures T_{YU} and T_{NY}, which are triggered at the first appearance of their respective curve type.

2.4.6. Optical characterization

T_{GM} corresponds to the test temperature, where a *fragile* fracture type occurs for the first time.

2.5. Overview transition temperatures

A compilation of all calculated transition temperatures is given in Table 3. With the exception of the glass fibre reinforced material M4, all materials follow similar trends between test standards and specimen thicknesses. Reproducibility, consistency and comparability are the main factors that need to be considered when evaluating the transition temperatures. At the same time, the calculations involved should be as simple as possible.

T_{30}^{Duc} shows the most inconsistent results because it is sensitive to noise of the force-deflection data after crack initiation.

Despite occasional outliers, the ISO characterization has proven itself to be an adequate representation of the transition regime with most of the other transition temperatures lying between the boundary values of T_{YU} and T_{NY}. For thin specimens, T_{NY} and T_{YU} stretch over a wide temperature range, which gets more narrow for thicker specimens.

In comparison to all the other categories, the fracture appearance usually gives much higher transition temperatures T_{GM}, because fractures are classified as brittle as soon as crack initiation is observed disregarding any plasticity that might be present before.

2.6. Transition shift factors

Since the trends of all categories are strikingly similar as can be seen in Table 3, the shift factors are contemplated to be universally applicable for all transition temperatures. However, the impact behaviour of glass fibre- and talcum reinforced PP-compounds is vastly different from the other tested materials. Consequently, only elastomer modified PP-grades (M1, M2, M3) as well as the most consistent transition temperatures (T^E, $T_{1.2}^{Rat}$, T^s) are used to determine the shift factors. For data extrapolation, 1 mm ISO test series are chosen as initial reference values, since 1 mm test series show the least standard deviations and ISO is generally more consistent than ASTM. This procedure is illustrated in Table 4. Finally, these shift factors are summarized in average values α, β, γ, δ, ϵ and ζ, which are listed in Table 5.

It should be pointed out, that the transition from ductile to brittle was not fully covered for the material M2, even at -70 °C, which is the reason why T^s values for M2ISOt2 and M2ISOt3 are assumed to be -70 °C.

	T^E	$T_{1.2}^{Rat}$	T^s	T_{30}^{Duc}	T_{NY}	T_{YU}	T_{GM}
M1ISOt1	-47	-50	-49	-35	-52	-30	-30
M1ISOt1	-57	-59	-57	-53	-58	-52	-50
M1ISOt3	-56	-56	-58	-55	-60	-56	-56
M1ASTMt1	-40	-29	-30	18	-40	-23	-30
M1ASTMt2	-47	-45	-50	-41	-50	-40	50
M1ASTMt3	-43	-43	-50	-36	-50	-50	-40
M1ASTMt4	-45	-45	-50	-41	-50	-50	-50
M2ISOt1	-50	-55	-50	-40	-	0	-20
M2ISOt2	-63	-66	-70	-56	-	-30	-30
M2ISOt3	-64	-65	-70	-	-	-40	-30
M2ASTMt1	-40	-36	-37	7	-	23	-20
M2ASTMt2	-55	-55	-60	-41	-	-40	-20
M2ASTMt3	-52	-50	-60	-43	-	-50	
M2ASTMt4	-54	-	-60	-22	-	-30	-30
M3ISOt1	-19	-20	-17	6	-30	-10	-20
M3ISOt2	-28	-29	-30	-8	-40	-10	-30
M3ISOt3	-26	-27	-25	-17	-34	-20	-30
M3ASTMt1	-23	-3	-10	16	-20	23	-10
M3ASTMt2	-26	-14	-19	5	-20	0	-10
M3ASTMt3	-26	-13	-19	7	-20	-10	-10
M3ASTMt4	-24	-	-28	-6	-30	-10	-20
M4ISOt2	-18	-	-	-	-	-	-
M4ISOt3	-7	-	-	-7	-	-	-
M4ASTMt1	-17	-	-17	-11	-	-	-
M4ASTMt2	-7	-27	-52	-27	-	-	-
M4ASTMt3	-6	-14	-5	-1	-	-	-
M4ASTMt4	5	-59	-22	6	-	-	-
M5ISOt1	-35	-35	-27	-4	-36	-10	-30
M5ISOt2	-36	-36	-36	-23	-38	-30	-40
M5ISOt3	-39	-	-36	-21	-50	-20	-40
M5ASTMt1	-35	-25	-21	11	-30	23	-30
M5ASTMt2	-35	-34	-30	-17	-40	-20	-30
M5ASTMt3	-34	-30	-39	-14	-40	-20	-30
M5ASTMt4	-27	-	-39	-12	-40	-20	-20

Table 3. Overview of all transition temperatures (all values in Celsius); nomenclature e.g. M3ISOt1: material M3, ISO test standard and 1 mm thick specimens.

	T^E	$T_{1.2}^{Rat}$	T^s
M1ISOt1	226 = x	223 = x	224 = x
M1ISOt1	216 = x · 0.955	214 = x · 0.959	216 = x · 0.964
M1ISOt3	217 = x · 0.960	217 = x · 0.973	215 = x · 0.959
M1ASTMt1	233 = x · 1.030	244 = x · 1.094	243 = x · 1.084
M1ASTMt2	226 = x · 1.000	228 = x · 1.022	223 = x · 0.995
M1ASTMt3	230 = x · 1.017	230 = x · 1.031	223 = x · 0.995
M1ASTMt4	228 = x · 1.008	228 = x · 1.022	223 = x · 0.995
M2ISOt1	223 = x	218 = x	223 = x
M2ISOt2	210 = x · 0.941	207 = x · 0.949	208 = x · 0.932
M2ISOt3	209 = x · 0.937	207 = x · 0.954	208 = x · 0.932
M2ASTMt1	233 = x · 1.044	237 = x · 1.087	236 = x · 1.058
M2ASTMt2	218 = x · 0.977	218 = x · 1.000	213 = x · 0.955
M2ASTMt3	221 = x · 0.991	223 = x · 1.022	213 = x · 0.955
M2ASTMt4	219 = x · 0.982		213 = x · 0.955
M3ISOt1	254 = x	253 = x	256 = x
M3ISOt2	245 = x · 0.964	244 = x · 0.964	243 = x · 0.949
M3ISOt3	247 = x · 0.972	246 = x · 0.972	248 = x · 0.968
M3ASTMt1	250 = x · 0.984	270 = x · 1.067	263 = x · 1.027
M3ASTMt2	247 = x · 0.972	259 = x · 1.023	254 = x · 0.992
M3ASTMt3	247 = x · 0.972	260 = x · 1.027	254 = x · 0.992
M3ASTMt4	249 = x · 0.980		245 = x · 0.957

Table 4. Determination of individual shift factors (all values in Kelvin).

	avg.	std.	
α	0.953	0.011	ISO1mm to ISO2mm
β	0.958	0.015	ISO1mm to ISO3mm
γ	1.053	0.035	ISO1mm to ASTM1mm
δ	0.993	0.022	ISO1mm to ASTM2mm
ϵ	1.000	0.026	ISO1mm to ASTM3mm
ζ	1.005	0.038	ISO1mm to ASTM4mm

Table 5. Average Kelvin temperature shift factors α, β, γ, δ, ϵ and ζ and their standard deviations.

The standard deviation of the shift factors listed in Table 5 become greater for thicker specimens. The predictions from 1 mm ISO to thicker ISO series shows accurate predictions, while extrapolations from ISO to ASTM generally hold higher deviations.

Figure 6 compares the predictions of the average shift factors with the results of the measured data.

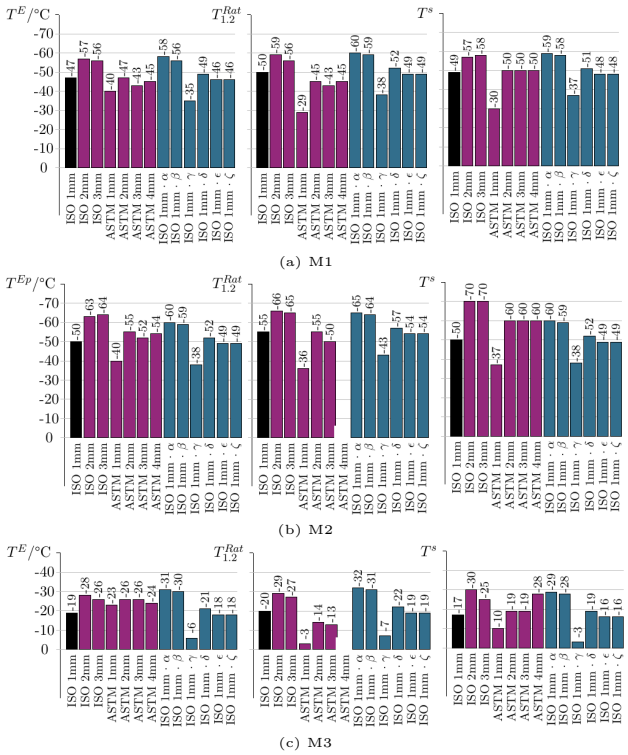

(a) M1

(b) M2

(c) M3

Figure 6. Shift factor predictions versus reality: The trend between ISO 1 mm (black) and thicker specimens (purple) can be predicted (blue) with temperature shift factors α, β, γ, δ, ϵ and ζ.

3. Conclusions

The experimental investigations show that transition temperatures for elastomer modified materials hold similar trends between test standards and specimen thicknesses. Temperature shift factors can be established to allow for the prediction of transition temperatures for elastomer filled PP at different testing conditions. While the data extrapolation is more consistent for ISO 6603-2 than ASTM D3763, satisfying values for all tested materials and conditions can be achieved. This may drastically reduce testing time, effort and costs and allow for comparison of data obtained by different test standards.

List of symbols

F_m Peak load [kN]
s_m Deflection at peak load [mm]
E_m Energy up to peak load [J]
F_p Puncture force [kN]
s_p Puncture deflection [mm]
E_p Puncture energy [J]
F_{yo} Initial force [kN]
s_{yo} Initial deflection [mm]
F_y Yield equivalent force [kN]
s_y Yield equivalent deflection [mm]
E_{el} Elastic energy portion [J]
E_{pl} Plastic energy portion [J]
k_{lin} Relative stiffness [N/mm]
Δs_w Width of plastic plateau [mm]
R_{el} Elastic energy ratio [–]
R_{duc} Ductility index [–]
s_{total} Total deflection [mm]
YD Yielding with deep drawing
YS Yielding with stable crack growth
YU Yielding with unstable crack growth
NY No yielding
T Temperature [°C]
T^E Transition temperature; puncture energy [°C]
$T^{Rat}_{1.2}$ Transition temperature; elastic energy ratio [°C]
T^{Duc}_{3o} Transition temperature; ductility index [°C]
T_{GM} Transition temperature; optical [°C]
T_{NY} Transition temperature; curve type NY [°C]
T_{YU} Transition temperature; curve type YU [°C]
$\alpha, \beta, \gamma, \delta, \epsilon, \zeta$ Average shift factors [–]

Acknowledgements

This research was supported by *Borealis Polyolefine GmbH* (Linz, A.)

References

[1] E. Baur, T. A. Osswald, N. Rudolph. *Saechtling Kunststoff Taschenbuch.* 31st printing. Carl Hanser Verlag, 2013.

[2] Plastics -Determination of puncture impact behaviour of rigid plastics - Part 2: Instrumented impact testing. ISO 6603-2, International Organization for Standardization, Geneva, Switzerland, 2000.

[3] Astm d3763-15, standard test method for high speed puncture properties of plastics using load and displacement sensors. *ASTM International* 2015. doi:10.1520/D3763-15.

[4] D. Huber. Temperaturgeführte Durchstoßprüfung von Kunststoffen - Vergleich von Durchstoßprüfmaschinen, Bachelor of Science, Montanuniversität Leoben, 2009.

[5] M. Böhning, U. Niebergall, A. Adam, W. Stark. Influence of biodiesel sorption on temperature-dependent impact properties of polyethylene. *Polymer Testing* **40**:133 – 142, 2014. doi:10.1016/j.polymertesting.2014.09.001.

[6] V. Hristov, R. Lach, W. Grellmann. Impact fracture behavior of modified polypropylene/wood fiber composites. *Polymer Testing* **23**(5):581 – 589, 2004. doi:10.1016/j.polymertesting.2003.10.011.

[7] A. Pavan, J. Williams. *Fracture of Polymers, Composites and Adhesives.* Volume 27. Elsevier Science, 2000.

[8] A. van der Wal, A. Wal, J. Mulder, R. Gaymans. Fracture of polypropylene: 2. the effect of the crystallinity. *Polymer* **39**(22):5477–, 1998. doi:10.1016/S0032-3861(97)10279-8.

[9] A. Wal, A. van der Wal, J. Mulder, et al. Polypropylene-rubber blends:1. the effect of matrix properties on the impact behaviour. *Polymer* **39**(26):6781–, 1998. doi:10.1016/S0032-3861(98)00170-0.

[10] A. van der Wal, A. Wal, R. Gaymans. Polypropylene-rubber blends 5: deformation mechanism during fracture. *Polymer* **1999**(40):6067–6067, 1999. doi:10.1016/S0032-3861(99)00216-5.

[11] C. Grein, K. Bernreitner, A. Hauer, et al. Impact modified isotatic polypropylene with controlled rubber intrinsic viscosities: Some new aspects about morphology and fracture. *Journal of Applied Polymer Science* **87**(10):1702–1712. https://onlinelibrary.wiley.com/doi/pdf/10.1002/app.11696 DOI:10.1002/app.11696.